Earth and Planetary Science Letters 602 (2023) 117929

Contents lists available at ScienceDirect

Earth and Planetary Science Letters

journal homepage: www.elsevier.com/locate/epsl

Porosity, strength, and alteration – Towards a new volcano stability assessment tool using VNIR-SWIR reflectance spectroscopy

Gabor Kereszturi [a,*], Michael Heap [b,c], Lauren N. Schaefer [d], Herlan Darmawan [e], Frances M. Deegan [f], Ben Kennedy [g], Jean-Christophe Komorowski [h], Stuart Mead [a], Marina Rosas-Carbajal [h], Amy Ryan [i], Valentin R. Troll [f], Marlène Villeneuve [j], Thomas R. Walter [k]

[a] Volcanic Risk Solutions, School of Agriculture and Environment, Massey University, Palmerston North, New Zealand
[b] Université de Strasbourg, CNRS, Institut Terre et Environnement de Strasbourg, UMR 7063, 5 rue Descartes, Strasbourg F-67084, France
[c] Institut Universitaire de France (IUF), Paris, France
[d] U.S. Geological Survey, Geologic Hazards Science Center, 1711 Illinois St., Golden, CO, 80401, USA
[e] Department of Physics, Faculty of Mathematics and Natural Sciences, Universitas Gadjah Mada, Yogyakarta, Indonesia
[f] Department of Earth Sciences, Section for Natural Resources and Sustainable Development (NRHU), Uppsala University, Sweden
[g] Geological Sciences, University of Canterbury, Christchurch, New Zealand
[h] Université de Paris, Institut de Physique du Globe de Paris, CNRS, Paris, France
[i] Department of Earth and Environmental Sciences, University of Minnesota, MN 55455, USA
[j] Subsurface Engineering, Montanuniversität Leoben, Leoben, Austria
[k] GFZ German Research Centre for Geosciences, Telegrafenberg, 14473 Potsdam, Germany

ARTICLE INFO

Article history:
Received 22 August 2022
Received in revised form 19 November 2022
Accepted 21 November 2022
Available online xxxx
Editor: C.M. Petrone

Keywords:
uniaxial compressive strength
advanced argillic alteration
debris avalanche
phyllosilicates
hyperspectral remote sensing
hydrothermal alteration

ABSTRACT

Volcano slope stability analysis is a critical component of volcanic hazard assessments and monitoring. However, traditional methods for assessing rock strength require physical samples of rock which may be difficult to obtain or characterize in bulk. Here, visible to shortwave infrared (350–2500 nm; VNIR–SWIR) reflected light spectroscopy on laboratory-tested rock samples from Ruapehu, Ohakuri, Whakaari, and Banks Peninsula (New Zealand), Merapi (Indonesia), Chaos Crags (USA), Styrian Basin (Austria) and La Soufrière de Guadeloupe (Eastern Caribbean) volcanoes was used to design a novel rapid chemometric-based method to estimate uniaxial compressive strength (UCS) and porosity. Our Partial Least Squares Regression models return moderate accuracies for both UCS and porosity, with R^2 of 0.43–0.49 and Mean Absolute Percentage Error (MAPE) of 0.2–0.4. When laboratory-measured porosity is included with spectral data, UCS prediction reaches an R^2 of 0.82 and MAPE of 0.11. Our models highlight that the observed changes in the UCS are coupled with subtle mineralogical changes due to hydrothermal alteration at wavelengths of 360–438, 532–597, 1405–1455, 2179–2272, 2332–2386, and 2460–2490 nm. These mineralogical changes include mineral replacement, precipitation hydrothermal alteration processes which impact the strength of volcanic rocks, such as mineral replacement, precipitation, and/or silicification. Our approach highlights that spectroscopy can provide a first order assessment of rock strength and/or porosity or be used to complement laboratory porosity-based predictive models. VNIR-SWIR spectroscopy therefore provides an accurate non-destructive way of assessing rock strength and alteration mineralogy, even from remote sensing platforms.

1. Introduction

The physical and mechanical properties of rocks at volcanoes are extremely diverse (e.g., Heap and Violay, 2021), resulting from their variable micro- and macrostructures. At the scale of a volcano, rocks with disparate physical and mechanical properties and heterogeneous structures are often found adjacent to each other (Manconi et al., 2007; Geshi et al., 2012; Mordensky et al., 2018a). This variation of structural characteristics is the result of original magma composition/primary mineralogy and eruptive activity, and can be further modified by mechanical stressing (Kendrick et al., 2013; Schaefer et al., 2015), shearing (Reid et al., 2010), thermal cracking (Vinciguerra et al., 2005; Fortin et al., 2011; Vasseur and

* Corresponding author.
E-mail address: G.Kereszturi@massey.ac.nz (G. Kereszturi).

https://doi.org/10.1016/j.epsl.2022.117929

Wadsworth, 2019), and alteration from magma migration and/or the circulation of hydrothermal fluids (Pola et al., 2012; Heap et al., 2019; Mordensky et al., 2019). As a result, a volcanic edifice is, mechanically, extremely heterogeneous on a variety of spatial and temporal scales.

Mechanical heterogeneities, over-steepened slopes, and topographic factors (Harnett and Heap, 2021), locally high pore fluid pressures (Reid, 2004; Heap et al., 2021a), hydrothermal veining (Mordensky et al., 2022), and alteration-induced weakening (van Wyk de Vries et al., 2000; Reid et al., 2001; Ball et al., 2018; Heap et al., 2021b; Darmawan et al., 2022) render volcanic edifices unstable and prone to potentially devastating collapse. These collapses may be triggered by magma intrusion, gas/fluid pressure, seismic activity, or even heavy rainfall. As volcano instability is thought to be closely associated with the occurrence and architecture of magma and hydrothermal pathways (Darmawan et al., 2018; Giampiccolo et al., 2020; Mordensky et al., 2022), understanding mechanical complexity forms an essential part of volcano monitoring. Modelling designed to assess the stability of a volcanic slope requires the knowledge of physical and mechanical properties of the edifice-forming rocks (Apuani et al., 2005; Schaefer et al., 2013; Harnett et al., 2018; Heap et al., 2021b; Kereszturi et al., 2021; Wallace et al., 2022). One such property, uniaxial compressive strength (UCS)—the maximum compressive stress a sample can support before failure when unidirectional stress is applied—is a commonly used metric to assess intact rock strength (Hoek and Brown, 1997; Heap and Violay, 2021). Although porosity exerts a first-order control on UCS, the strength of volcanic rocks at a given porosity can vary significantly due to microstructural diversity (e.g., pore, shape and distribution) (Bubeck et al., 2017; Griffiths et al., 2017) and variations in alteration intensity and/or crystal content and size (Fig. 1A-B) (Heap and Violay, 2021; Darmawan et al., 2022).

Transformative change in the study of volcano slope stability assessments is possible if an independent variable—one that is quick and/or easy to measure—can be used to estimate the UCS and porosity of volcanic rocks. UCS experiments require specialised and expensive laboratory equipment. Additionally, blocks (potentially subjected to sampling ethics) must be transported to the laboratory and samples then need to be prepared with precise geometries, which is a time-consuming process. In contrast, field-based or remote sensing measurements that do not require sample collection, laboratory preparation, or laboratory testing could more rapidly estimate surficial rock physical and mechanical properties and their distribution. This could be used as input parameters in stability models in near-real-time and could therefore provide volcano observatories with more timely first-order stability assessments. Measuring rocks in-situ additionally bypasses complex sample retrieval issues when assessing the mechanical heterogeneity of a volcano, such as highly altered or fractured material which by their nature are often delicate, friable, and difficult to prepare for laboratory analysis. Recent efforts in this direction have shown that rock physical and mechanical properties can be estimated using the percentage by weight (wt.%) of secondary alteration minerals (Heap et al., 2021b), rapid, non-invasive reflectance spectroscopy (Schaefer et al., 2021), and whole-rock oxygen isotopes (Darmawan et al., 2022; Heap et al., 2022) and cation exchange capacity (Revil et al., 2022).

Reflectance spectroscopy has become increasingly used to explore soil and rock types by spectral band analysis, such as in the visible and near-infrared (350–1000 nm; VNIR), shortwave infrared (1000–2500 nm; SWIR) and thermal infrared (7000–13000 nm; TIR) bands relevant for hydrothermal alteration mapping (Rowan et al., 2003; Darmawan et al., 2018; Kereszturi et al., 2018; Müller et al., 2021). In particular, those alteration zones including iron oxide, as well as argillic, phyllic, and propylitic alterations minerals, can be identified using both multispectral (Loughlin, 1991; Rowan et al., 2003) and hyperspectral data (Clark et al., 2003; Neal et al., 2018; Kereszturi et al., 2020; Thiele et al., 2022). Airborne, drone-based or carry-on devices can also effectively map physico-chemical changes of volcanic rocks and, when combined with effective processing algorithms (e.g., Partial Least Squares Regression) that can handle collinearity and high dimensionality (e.g., Wold et al., 2001), they can become effective platforms for characterising the mineralogy and alteration of volcanic rocks.

Here, we present the results of a study designed to estimate UCS and porosity of hand-samples using a VNIR–SWIR reflectance spectroradiometer. One of the advantages of VNIR–SWIR spectroscopy is that it is sensitive to both the physical (e.g., crystal or particle size, scattering due to surface roughness) and chemical (e.g., mineral composition and abundance) properties of rocks. Our aim is to provide a new, fast, and inexpensive method to estimate important physical and mechanical properties of fresh to variably hydrothermally altered volcanic rocks, assisting with robust volcanic hazard assessments.

2. Study design and method

We analysed laboratory-tested samples from a variety of volcanic settings, comprising Ruapehu, Ohakuri, Whakaari, and Banks Peninsula (New Zealand), Merapi (Indonesia), Chaos Crags (USA), Styrian Basin (Austria), and La Soufrière de Guadeloupe (Eastern Caribbean), which together represent the full spectrum of compositions from basaltic to rhyolitic (Table S1). In the database, each sample represents either a single core or the arithmetic means of multiple cores where available (Table S1). These samples have been previously characterised in terms of field relationships, their total porosity (henceforth referred to as “porosity”), and destructive UCS testing (Heap et al., 2015, 2017; Mordensky et al., 2018a, 2018b, Heap et al., 2019; Mordensky et al., 2019; Heap et al., 2020, 2021a, 2021b; Darmawan et al., 2022; Schaefer et al., 2022). The porosity was measured by using a helium pycnometer (Micromeritics AccuPyc II 1340; Heap et al., 2020), while the UCS was measured using a uniaxial load frame (Heap et al., 2020). Our samples show little to no isolated porosity; thus the predictions may not work well if the rocks contain a lot of isolated porosity.

We performed reflectance spectroscopy measurements on powdered rock (n=117) and rock chip samples (n=93) using a FieldSpec 4 Hi-Res NG spectroradiometer. While measurements were made on pre-collected rocks and thus were measured in the laboratory, the FieldSpec 4 is fully portable and capable of making the same measurements in a field setting. A Hi-Brightness contact probe with 10 mm footprint was used. Samples were powdered with a tungsten carbide benchtop ring mill to reduce the alteration rim-effects on the spectroscopy measurements, and to homogenise the samples (typically grain size of $\leq$500 μm). The rock chip samples were broken into smaller pieces to expose internal parts using a hammer. Both the internal and external portions of the rock chips were measured to produce spectral measurements that are representative of the whole-rock composition. The spectral measurements were collected between 350–2500 nm at 2151 spectral bands, with 1 nm spectral sampling and bandwidth of 1.4 nm at 350–1000 nm, and 1.1 nm at 1001–2500 nm. The spectral readings were calibrated against a white Spectralon Diffuse Reflectance Standard. In total, 3–5 spot measurements of each sample were taken to ensure a good representation of the overall mineralogy. The spectral measurements were splice-corrected to remove sensor shift artefacts, and averaged, following previous studies (Schaefer et al., 2021).

The reflectance spectra (Fig. S1) were continuum removed, which eliminates the background intensity and normalises the data for absorption features by fitting a convex hull to the spectral re-

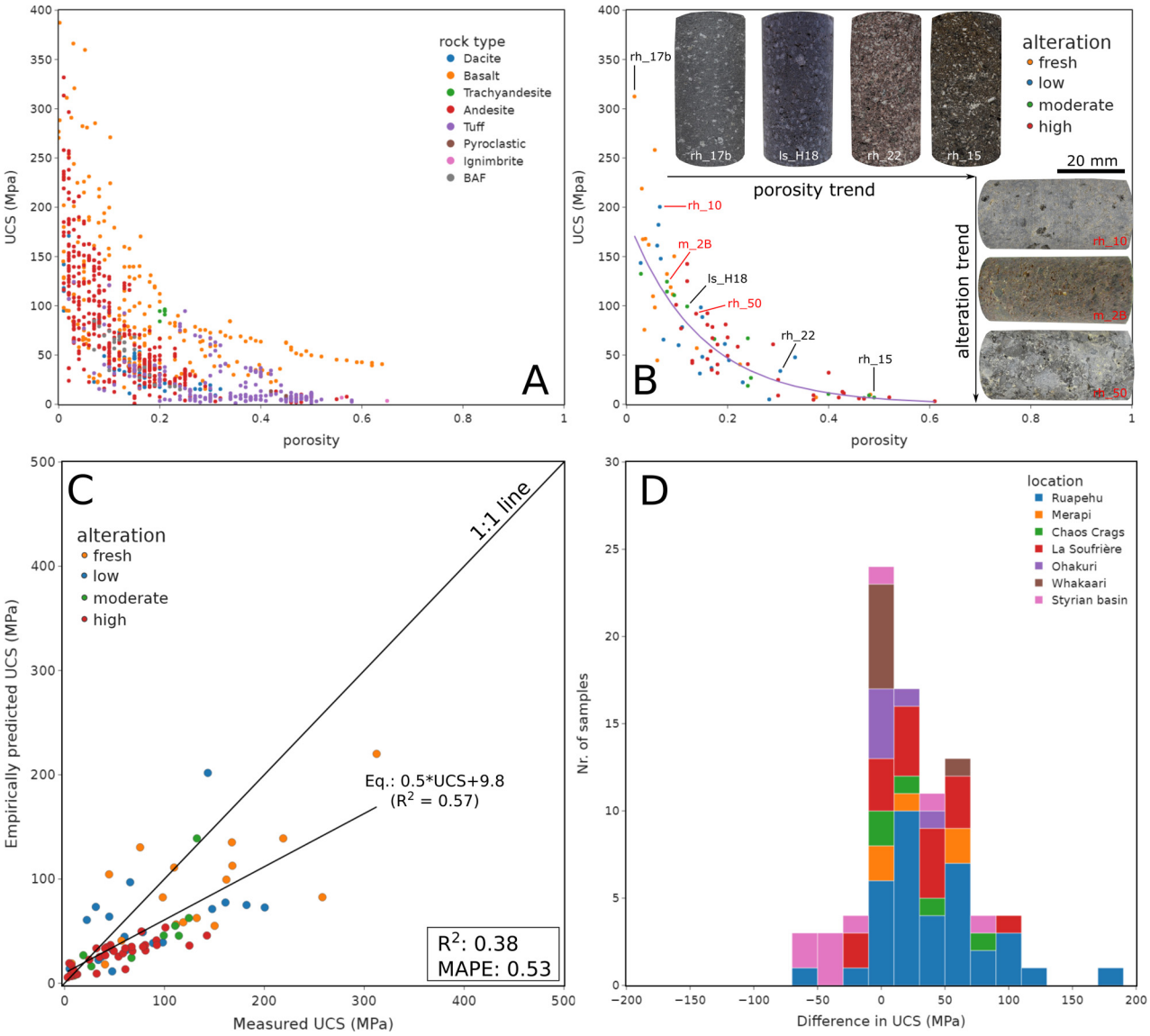

Fig. 1. (A) Uniaxial compressive strength (UCS) as a function of porosity for different volcanic rock types. Dacite, Basalt, Trachyandesite and Andesite refer to lava, while the rest refer to pyroclastic rocks (after Heap and Violay (2021)). (B) UCS as a function of porosity for the dataset presented in this study, coloured by the degree of alteration, with insets showing photographs of select sample cores. The photographs provided showcase porosity- and alteration-driven changes in UCS. The examples included in the alteration trend have roughly the same porosity between 0.07 and 0.14. (C) Plot of measured and empirically predicted UCS using Eq. 14 in Villeneuve and Heap (2021). Note the strong deviation for most data points from the 1:1 line. Equation denotes best fit of the empirical vs. measured UCS data. (D) Error histogram showing the strong underestimation of UCS.

flectance curve (Clark et al., 1990). The continuum removed spectra were further smoothed using Savitzky-Golay filtering (Savitzky and Golay, 1964) with a first-order polynomial on a 5 band-wide window with no derivatives. Further pre-processing included (1) elimination of the first and last 10 bands to reduce instrumental and environmental noise; (2) log-transformation to reduce skewness for both X and Y data; and (3) data standardisation by centering and scaling to unit variance for predictor variables X only (e.g., spectral reflectance data).

In this work, we applied the Non-linear Iterative Partial Least Squares (PLSR) algorithm, implemented in *sklearn* package (Pedregosa et al., 2011), for predicting porosity and UCS independently (Fig. S2A). PLSR is an effective method to maximise the covariance structures between two matrices, X and Y, through orthogonal matrix decomposition (Wold et al., 2001). PLSR is an appropriate method since moderate to strong correlations can be inferred between the individual spectral bands (e.g., sensitive to primary and secondary mineralogy) and rock mechanical properties, because hydrothermal alteration manifest as secondary mineral precipitation and dissolution affects rock strength and stiffness (Schaefer et al., 2021). Furthermore, PLSR can handle strongly collinear and noisy data where the predictor-variables often outnumber the number of samples, a common case for spectroscopy data with thousands of bands. PLSR transforms the X matrix to a user-defined lower dimensional space but maintains the data structure while maximizing the correlation between the X and Y matrices. The models were validated using repeated K-fold cross-validation (CV), a procedure used to assess how the results of a statistical analysis will generalize to an independent data set, where k=5 with 100 repeats (Fig. S2). The k=5 ensures adequate number of validation samples at each split (ca. 20–25 samples). The number of PLS components for each model was selected by fitting models with up to 20 components iteratively and measuring the Mean Absolute Percentage Error (MAPE). The models with the

lowest MAPE were selected for predicting rock mechanical properties.

Nested prediction models were also trialled to predict UCS only using a combination of spectral and either PLSR-predicted or laboratory-measured porosity data as *X* (Fig. S2B). The spectral data were transformed using Principal Component Analysis (PCA); PCA was preferred to avoid data leaking and overfitting (Kaufman et al., 2011) since it is an unsupervised method (i.e., requires no *Y* variables). The first 6–9 principal components were used, corresponding to 94–96% of the variance in the spectral data (Fig. S2), selected on a trial-and-error basis. The final UCS predictions were made with a Support Vector Regression (SVR). The Radial Basis Function kernel was used with a constant epsilon of 0.1. The gamma (controls model complexity) and C (regularization term to fight over-fitting) parameters were estimated using a regular grid-search (C: 1, 10, 20, 50, 75, 100 and gamma: 0.0001, 0.001, 0.01, 0.1, 1) with repeated K-fold cross-validation (k=5, repeat = 100). The C and gamma parameters with the lowest MAPE were used (Fig. S2).

All models were validated using R^2 and MAPE. R^2 is a unitless error metric, with values spanning from 0 to 1, where 1 means a perfect 1:1 match between predicted and measured values. R^2 can have negative values, indicating when the predictions do not follow any trend of the measured data. MAPE has been chosen to quantify the average error in percentages, since prediction errors are expected to change by magnitude of the input data. The values closer to zero are better.

For each PLSR model, the locations of the important spectral bands were calculated using the Variable Influence on Projection (VIP) method (Wold et al., 2001), with values ranging from 0 to infinite. The average squared values of VIP scores for each band equals 1, thus values above this threshold are considered to contribute more to the prediction (Chong and Jun, 2005). However, the actual threshold depends on the number of important and unimportant predictor variables, magnitude of correlation between predictors, signal to noise ratio and the structure of the regression coefficients (Chong and Jun, 2005). Thus, we estimated this level to be at 1.2 in our case. Spectral bands with VIP score >1.2 are therefore of particular interest to understand the causality of the PLSR model prediction and to link the prediction with underlying physical and chemical processes.

3. Porosity and UCS predictions for volcanic rocks

PLSR models for porosity and UCS were developed with PLS components between 5–8, with fewer components for predictions based on the powdered samples. Conceptually, the powder-based predictions should perform better than the rock-based models, due to a more homogeneous mixing of primary and alteration mineralogy and grain size. However, our rock-based PLSR models for both UCS and porosity perform, within the same range as models developed on powdered samples (R^2 ~0.43–0.49 and MAPE ~0.20–0.40; Table 1), although with more complex underlying prediction models (e.g., more PLS components; Table 1).

The PLSR models show a heteroskedasticity behaviours, with large scatter towards larger UCS and porosity values (Figs. 2 and 3). The PLSR predictions for UCS ($R^2 = 0.43$, MAPE=0.20; Table 1) yield at least similar accuracy metrics as the empirically predicted UCS using laboratory measured porosity ($R^2 = 0.38$, MAPE=0.53; Table 1 and Fig. 1C); however, with a significant reduction in MAPE. Interestingly, the spectroscopy-based PLSR predictions for both porosity (Fig. 2) and UCS (Fig. 3) can further 'correct' for the underestimation observed in empirically calibrated models (Figs. 1D and 3D). Thus, our results confirm that VNIR–SWIR reflectance can be a valuable addition to physical and rock mechanical testing.

The complex 'nested' models for UCS using both spectroscopy and porosity performed better than single PLSR models using spectroscopy only, regardless of whether porosity was predicted via spectroscopy ('low accuracy') or measured in the laboratory ('high accuracy') (Fig. 4 and Table 1). This further reinforces the important role that porosity plays in governing the UCS of volcanic rocks (e.g., Heap and Violay, 2021; Darmawan et al., 2022). The best performing UCS model is predicted via PCA-SVR with measured porosity data, which increased the predictions as high as $R^2 = 0.82$ (Table 1). This also vastly improves MAPE from 0.20 to 0.11, however, it also increases the model complexity (e.g., number of input variables).

4. Discussion

4.1. Underlying geological processes influencing UCS and porosity

To fingerprint geological processes impacting our UCS and porosity predictions, VIP scores have been calculated for all PLSR models developed on the full dataset. The VIP scores plotted as a function of wavelength can highlight spectral regions that contribute more than the average to the prediction (Fig. 5). UCS and porosity are well correlated (e.g., Fig. 1B), and both UCS and porosity models have very similar VIP curves, while differences only exist between the rock chip and rock powder-based models (Figs. 5A and B). The position of VIP >1.2 corresponds broadly to the absorption features of primary and secondary minerals (Fig. 5C).

The largest difference in VIP score between rock and powered rock models appears at 360–438 and 532–597 nm as well as at 2333–2387 nm (Figs. 5A and B). The former region, corresponding to electronic transition in Fe-rich minerals (e.g., Hunt, 1977), shows importance only for rock-based models, while the latter region becomes important for powder-based predictions. The absorption at 360–438 and 532–597 nm with a broad minor peak (VIP < 1.2) at ca. 1000 nm can be linked to goethite/hematite/ferrihydrite, and some primary minerals, such as olivine and pyroxenes, due to Fe in their crystal lattice (Bishop et al., 2017). Based on X-ray powder diffraction, Scanning Electron Microscopy with Energy Dispersive X-ray spectroscopy, and reflected light spectroscopy, goethite and hematite occur abundantly in the analysed samples as alteration rims and as oxidation products from Fe-bearing minerals (e.g., pyrite) (Heap et al., 2017; Mordensky et al., 2019; Kereszturi et al., 2020; Heap et al., 2021a; Schaefer et al., 2022). Therefore, we interpret these minerals as the main mineral phases that drive the UCS and porosity predictions within the VNIR region. Furthermore, the lack of VIP >1.2 in the powder models also suggest that alteration rims and rock texture carry diagnostic spectral information that better reflect rock strength and porosity, which is lost when testing powdered samples.

In contrast, absorption features at 2332–2386 nm and a minor peak at 2296–2316 nm in volcanic rock are important for powder-based predictions only. This region is characteristic of primary mineralogy (e.g., plagioclase series at 2332–2386 nm and pyroxenes at 2296–2316 nm), and alteration minerals, arising from propylitic alteration (e.g., epidote, chlorite, K-feldspar or white mica) (Neal et al., 2018) and kaolinite with Fe- and/or Mg impurities (Madejová et al., 2017). None of the samples contain propylitic alteration minerals, although, some samples from Ohakuri (n=5) and Chaos Crags (n=5) have been subject to silicification and K-feldspar alteration and contain kaolinite and smectites (typically ≤6 wt.%; (Heap et al., 2020, 2021a). Thus, mostly primary mineralogy should be responsible for this zone of VIP >1.2 in this dataset, which has been enhanced by reducing the vol.% of rim alteration and increasing exposure of primary minerals through powdering.

The remainder of the high VIP scores occur in the SWIR at 1405–1455, 1889–2014, 2179–2272, and 2460–2490 nm (Fig. 5),

Table 1
Model performance metrics for uniaxial compressive strength (UCS) and porosity predictions. Abbreviations: comp. – components in the models, PLS – Partial Least Squares or latent variables, PCA – Principal Component Analysis, SVR – Support Vector Regression, R^2 – R^2 coefficient of determination, MAPE – Mean Absolute Percentage Error, K-Fold CV – K-fold Cross Validation.

input	parameters	model	samples	comp.	R^2	MAPE (fraction)
rock spectra	porosity (fraction)	PLSR	88	8 PLS	0.44	0.29
	UCS (MPa)	Empirical model	85	-	0.38	0.53
		PLSR	90	8 PLS	0.43	0.20
		PCA-SVR - porPred	85	9 PLS and 7 PCA	0.47	0.20
		PCA-SVR - porMeas		6 PCA	0.82	0.11
powder spectra	porosity (fraction)	PLSR Kfold	112	5 PLS	0.43	0.40
	UCS (MPa)	PLSR Kfold	113	5 PLS	0.49	0.31

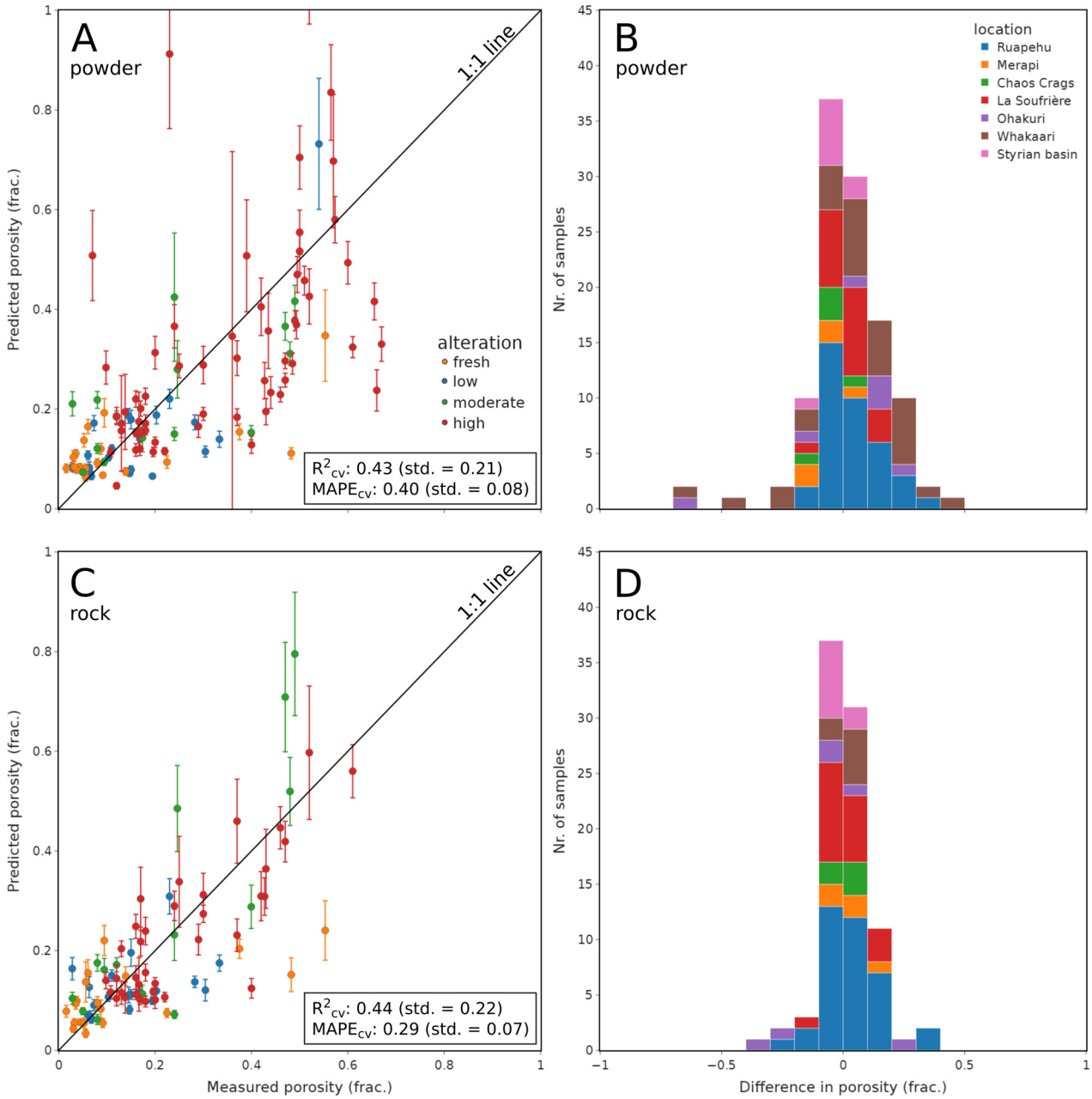

Fig. 2. Porosity predictions with Partial Least Squares Regression (PLSR) using rock powder (A-B) and rock chips (C-D). A and C show the measured versus predicted values, while B and D display the difference between the predicted and measured porosity. The plots shown here are from the K-fold cross validation (K-fold CV). Both B and D show a moderate underestimation of porosity using spectroscopy. The error bars show 1 standard deviation from the repeated (n=100) K-fold CV.

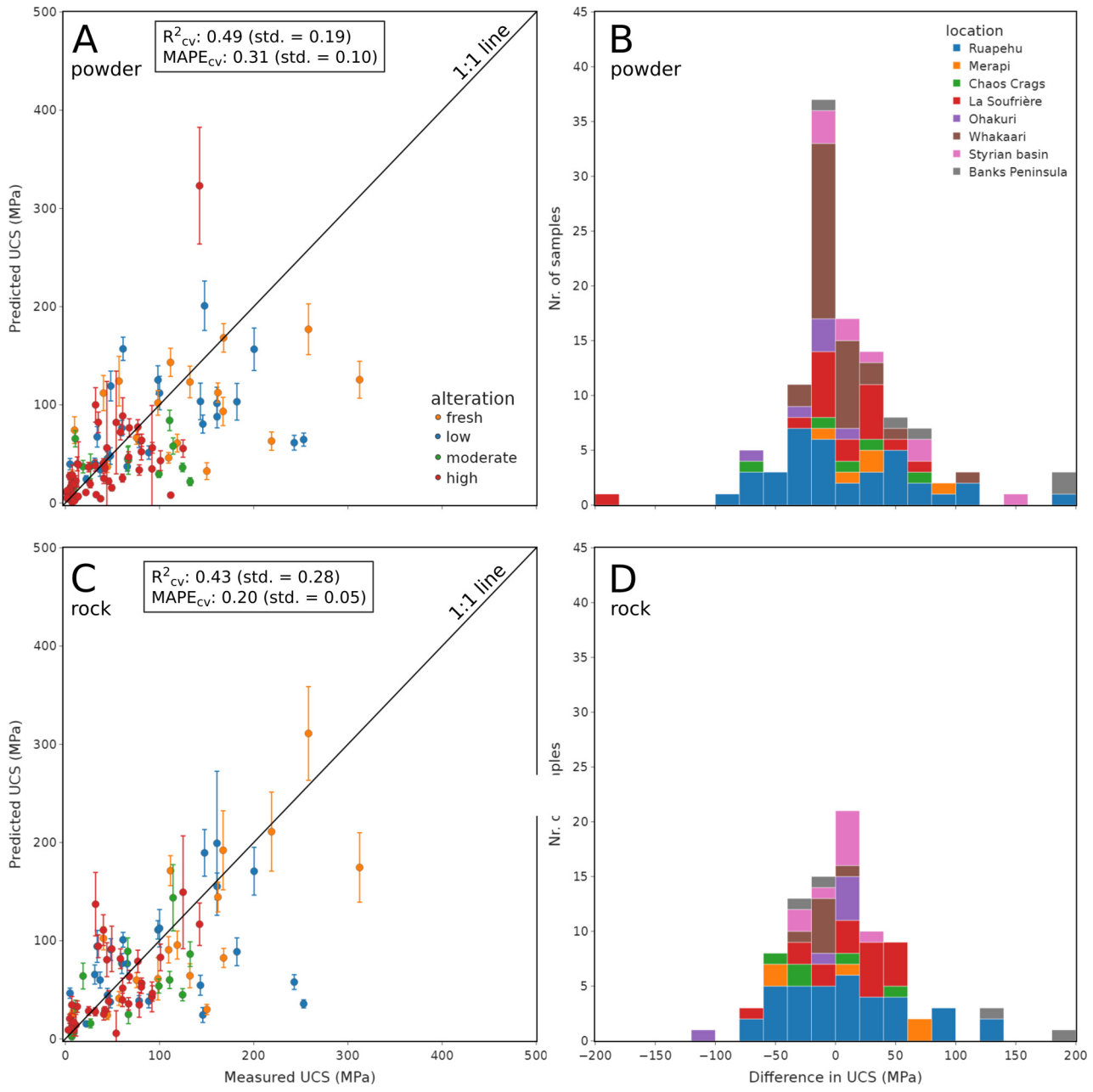

Fig. 3. Uniaxial compressive strength (UCS) prediction with Partial Least Squares Regression (PLSR) using rock powder (A-B) and rock chips (C-D). A and C show the measured versus predicted values, while B and D display the difference between the predicted and measured porosity. The plots shown here are from the K-fold cross validation (K-fold CV). Note D shows an improved prediction with less underestimation of UCS. The error bars show 1 standard deviation from the repeated (n=100) K-fold CV.

which is consistent with the stretching and bending of molecular OH, H_2O, SO_4, and M-OH, where M is a metal cation, such as Al, Mg, Fe^{2+}, and Fe^{3+} (Madejová et al., 2017). Our samples have typically intermediate to advanced argillic mineral associations of varying amounts of kaolinite, smectite, alunite, quartz polymorphs, gypsum/anhydrite, sulphur, barite, pyrite, and Fe-oxides (Heap et al., 2017; Mordensky et al., 2019; Kereszturi et al., 2020; Heap et al., 2021b; Darmawan et al., 2022), which can produce the observed absorption features at those VIP >1.2 regions (Fig. 5). Advanced argillic alteration can exert a strong control on both porosity and UCS (Pola et al., 2012; Frolova et al., 2014; Heap et al., 2021b) through the dissolution and precipitation of secondary minerals (Heap et al., 2015; Kanakiya et al., 2021). The presented UCS and porosity prediction model, therefore, adaptively corresponds to this complex physical and chemical evolution of volcanic rocks subject to hydrothermal alteration, through the sensitivity of the VNIR-SWIR data. Lastly, the PLSR predictions using VNIR-SWIR spectral data can better explain the UCS changes than porosity-based empirical models with MAPE of 0.20 and 0.53, respectively.

Besides the most prominent absorption feature around 1889–2014 nm due to molecular water (e.g., interlayer crystalline water), all other VIPs >1.2 are located on the margin of absorption features (e.g., 360–438, 532–597, 1405–1455, 2179–2272, 2332–2386, and 2460–2490 nm) of alteration minerals typical of advanced argillic alteration (black arrows in Fig. 5C). The exact position of an absorption feature (i.e., wavelength of the deepest feature) can be diagnostic to the sample mineralogy. However, the position is also sensitive to any grain size, occurrence (e.g., intimate and granularly mixed minerals), crystal lattice orientation, and metal cation substitution (Bishop et al., 2002; Clark et al., 2003), resulting in spectral shifts. Hence, the association of VIPs with absorption features highlights the importance of alteration min-

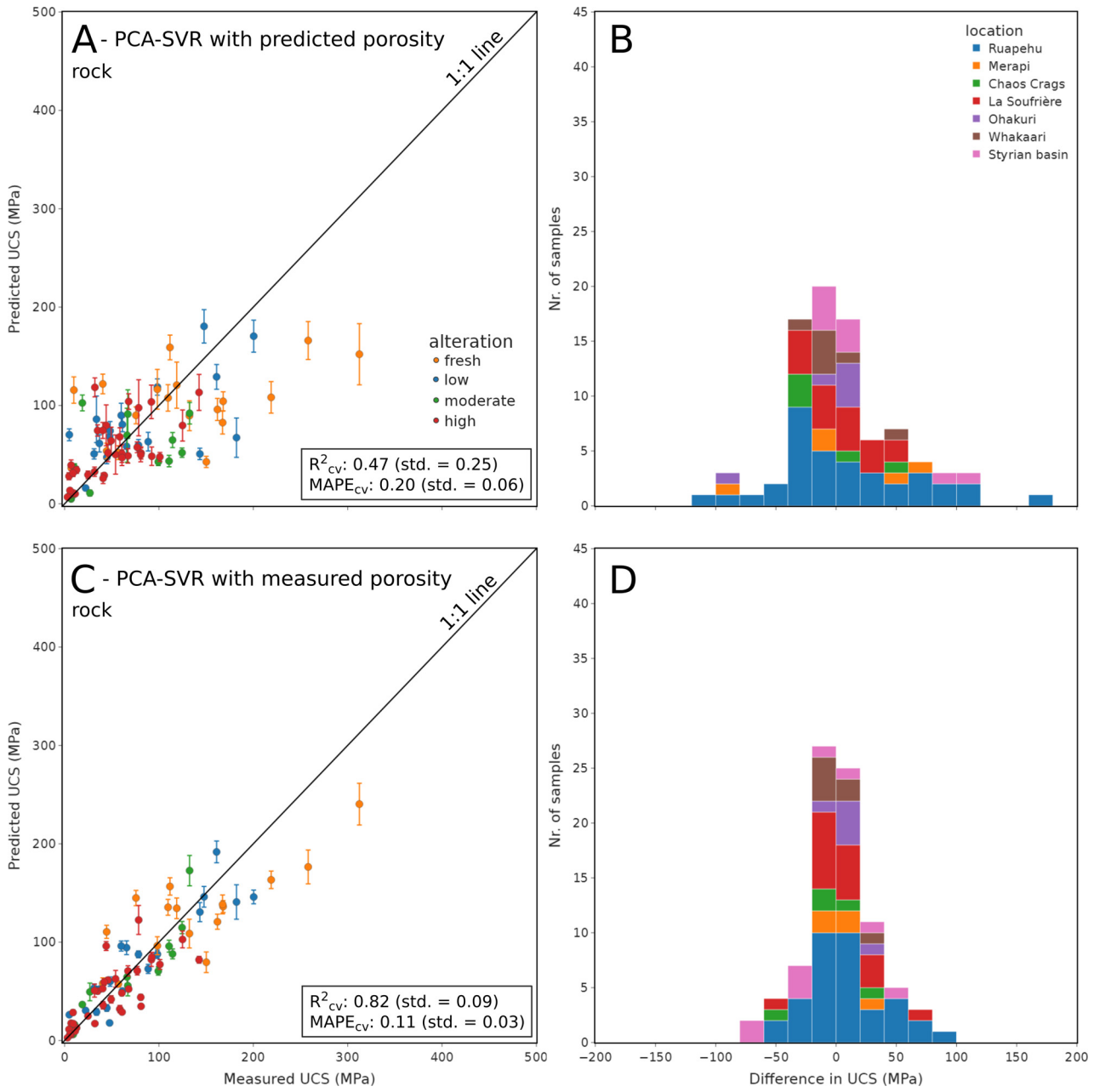

Fig. 4. Nested models for uniaxial compressive strength (UCS) prediction using Partial Least Squares Regression-predicted porosity (A-B) and laboratory-measured porosity (C-D). The error bars show 1 standard deviation from the repeated (n=100) K-fold cross validation.

eralogy and their interlayer molecular water and metal cation substitutions. The shape of the reflectance curve (e.g., steepness and secondary absorption features) is thus more informative about the mechanical behaviour of volcanic rocks than the presence or absence of a specific alteration mineral phase alone (e.g., kaolinite, alunite). The proposed PLSR prediction models can successfully generalise based on this systematic behaviour to estimate UCS and porosity.

4.2. Model complexity, variability, and bias of UCS

Prediction models for UCS using machine learning and deep learning approaches have widely been developed for travertines (Barzegar et al., 2016), sandstones (Jahed Armaghani et al., 2016a), and granite (Jahed Armaghani et al., 2016b). These models often reach R^2 of 0.65–0.95 and a mean absolute error of 1–5 MPa, outperforming our models. However, previous models consider either monomineralic rocks, rocks with a low mineralogical diversity, or rocks with a narrower range of porosity. Furthermore, the samples in these earlier studies are unaltered and are predicted using 'expensive' and highly correlated predictor variables (e.g., crystal content, point load index, Schmidt rebound hardness, Shore hardness, elastic wave velocity, density, permeability). In contrast, our database of volcanic rocks is characterised by heterogeneous primary textures and mineral assemblages with variable crystallinities, complex eruption/alteration histories, and variable and complex pore structure and microfractures. Despite these interacting properties, which increase model complexity for predicting UCS, our models show the potential to capture complex UCS changes (R^2 = 0.43 and MAPE=0.20). Additionally, our models can capture these complex UCS relationships independently of whether the change is controlled by porosity or (hydrothermal) alteration.

Each spectral band can only be moderately correlated with the mechanical and physical properties of volcanic rocks (Schaefer et

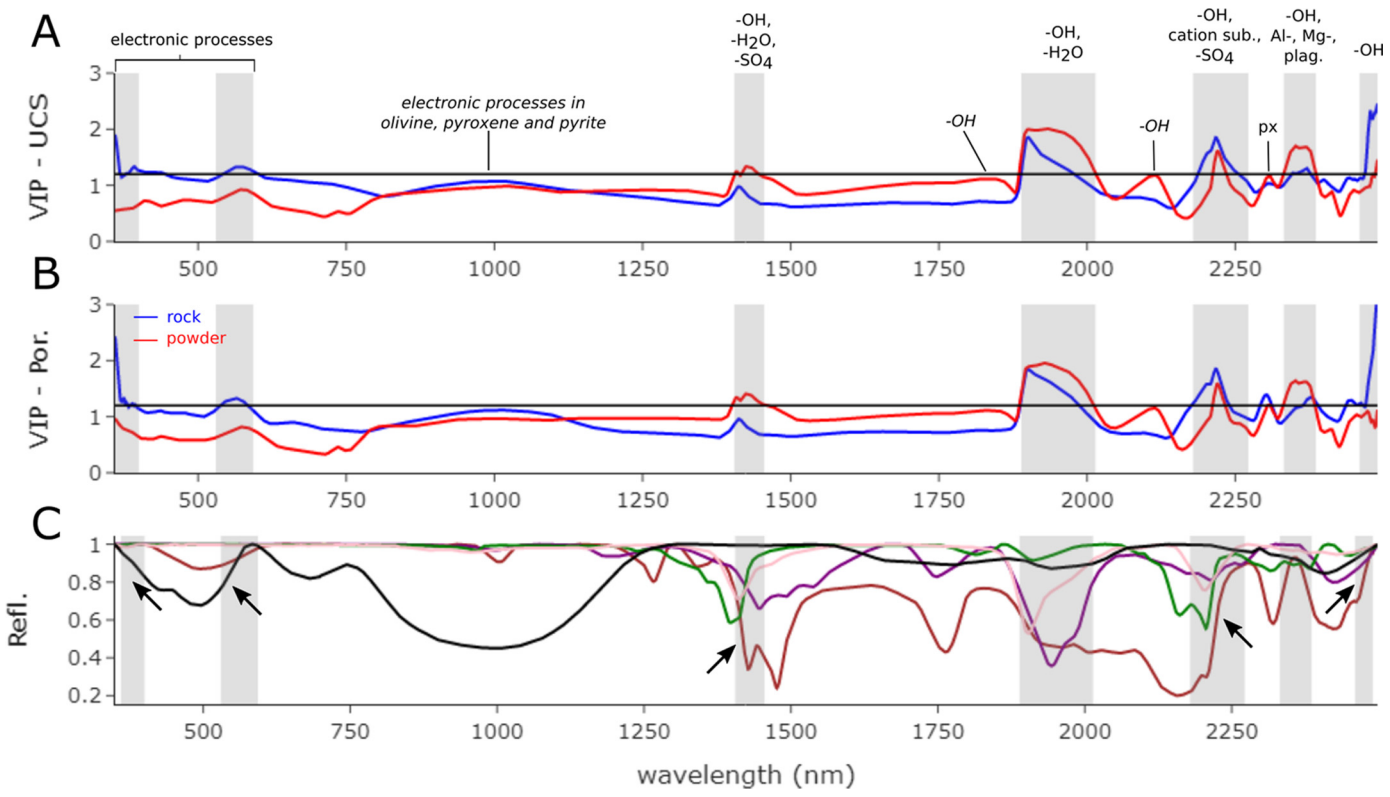

Fig. 5. Variable Influence on Projection (VIP) plots with important spectral regions (grey areas) with VIP >1.2 (black horizontal line on A and B) for uniaxial compressive strength (UCS) and porosity models (A and B). The blue line indicates rock samples, and the red line indicates powder samples. Continuum-removed VNIR–SWIR reflectance spectra are shown for typical alteration minerals for advanced argillic alteration (C). The grey areas correspond to various vibrational features due to stretching and/or bending (abbreviations: cation sub. – cation substitution; plag. - plagioclase; px. - pyroxene). Black arrows show when VIP >1.2 occurs at the shoulder of the light absorption feature. Data in (C) is from USGS spectral Library (Kokaly et al., 2017), where colours correspond to different minerals: brown –'AluniteHS295.4B', purple –'GypsumSU2202', green –'KaoliniteCM9', pink –'MontmorilloniteCM26', black –'GoethiteWS222CoarseGr'. (For interpretation of the colours in the figure(s), the reader is referred to the web version of this article.)

al., 2021). However, multivariate statistical models can maximise the predictive power of VNIR–SWIR reflectance. These models can adequately capture the variations in physical and chemical properties between samples. Since the underlying model complexity can be generalised to predict rock mechanical properties on samples that have not been used in the model training (i.e., "unseen" samples), the resultant UCS prediction models can effectively decouple the UCS prediction error from porosity and hydrothermal alteration processes. This feature can help to resolve the complexity and intimate relationship between these common rock mechanical attributes in volcanic systems.

The UCS predictions are subject to uncertainty due to the sampling bias of the database presented here, which is somewhat imbalanced (e.g., most samples are from andesitic composite volcanoes, which, tend to host argillic alteration). Consequently, we prefer repeated K-fold CV to validate the prediction models which can return sample UCS, and porosity estimates within each fold and each repetition. Any large deviations can then highlight how 'easy' it is to predict UCS and porosity using VNIR–SWIR reflectance data with reference to the training data. To visualise the variability of our predictions we selected two samples from the Ohakuri ignimbrite (Fig. 6) and compared them with individual UCS experiments (Heap et al., 2020).

One example, o_OI2B, has been predicted with a small bias by PLSR using only spectral data but, when porosity was included, the PCA-SVR models accurately predicted both the mean and the range (n=6) of the individual UCS experiment results (Fig. 6A–C). Sample o_OI2B can therefore show the importance of (initial) porosity on UCS, given that this sample is only a moderately altered ignimbrite with only 6 wt.% of phyllosilicates and zeolites (Heap et al., 2020). It is also worth noting that most UCS predictions are within the range of the laboratory measurements. Hence, our prediction models can be used to estimate the natural variability of UCS within volcanic rocks without extra sampling efforts (e.g., field-based surveys), if the unseen rock sample matches spectrally and mineralogically with the database presented in this study.

An extreme case, o_OI2A, shows the narrower variability of UCS when porosity is included, but at the expense of bias (Fig. 6D–F). Sample o_OI2A is a highly altered ignimbrite, which contains 53 and 47 wt.% of K-feldspar (e.g., adularia) and quartz, respectively (Heap et al., 2020). Furthermore, its hydrothermal alteration has demonstrably increased its UCS by replacing primary mineralogy with stronger quartz polymorphs (Heap et al., 2020). In this case, UCS estimates from each cross-validation folds and repeats match reasonably well with the laboratory UCS experiments (n=13) for the PLSR model (Fig. 6D). However, including porosity has led to an underestimation of the UCS and increasingly biased estimates (Fig. 6E and F). This can be explained by the lack of characteristic absorption features for quartz and adularia in the VNIR-SWIR. Lithologies with silicification should therefore be treated carefully when estimating their UCS using VNIR-SWIR reflectance spectroscopy.

4.3. Implications for (volcano) slope stability analysis

The combination of deposit emplacement and alteration history in volcanic environments can create a heterogeneous rock mass in terms of the distribution of rock physical and mechanical properties and fractures. In any slope stability assessment, sampling can often be subjected to bias and problems associated with field ac-

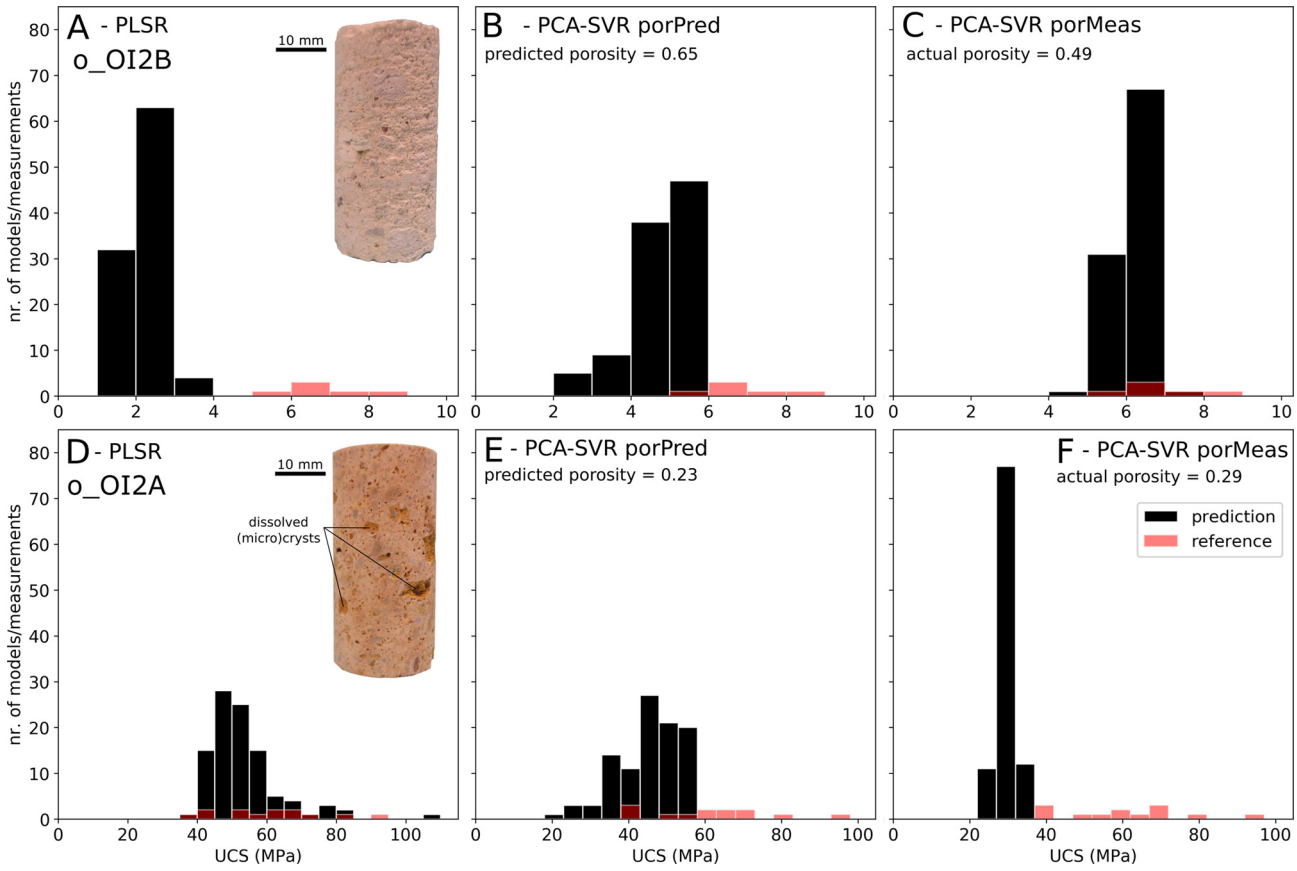

Fig. 6. Distribution of uniaxial compressive strength (UCS) estimates from each fold and repeats of cross-validation showing matching variability with laboratory UCS experiments. Two samples from the Ohakuri ignimbrite are shown: o_OI2B (upper row) and o_OI2A (lower row) and photographs of the samples are provided on panels A and D, respectively. The laboratory data for UCS and porosity are from Heap et al. (2020). Acronyms: PLSR – Partial Least Squares Regression; PCA – Principal Component Analysis, SVR – Support Vector Regression.

cessibility. As a result, laboratory studies often fail to resolve the immense natural heterogeneity that characterises volcanic edifices. Our prediction models using spectroscopic techniques can potentially overcome such a challenge since the models can also be applied to mechanically untested samples that share similar spectral and mineralogical characteristics to the dataset used in the training process.

Applying our PLSR prediction models using the full dataset with seven volcanoes reveals the spatial variability of UCS and porosity. As a demonstration, we have applied PLSR-based models to a natural outcrop within the 166–80 ky-old Wahianoa Formation (Gamble et al., 2003) on Mt Ruapehu, New Zealand (Fig. 7A). Only one sample, r_rh38, corresponding to this lithological unit has been sampled for mechanical testing, returning a UCS of 81 MPa and a porosity of 0.2 (Schaefer et al., 2022), while other samples have been collected for spectral analysis. Our model predictions of both UCS and porosity scatter around the UCS and porosity of the mechanically tested sample r_rh38 (Fig. 7A). Even though our models on these untested samples are only validated semi-quantitatively, the untested samples originate from a spectrally similar population to the training data (Fig. 7B). Therefore, the models can provide a new and powerful tool, providing strength estimates of locations on volcanoes for which laboratory testing is not available or feasible. Furthermore, the spectroscopy approach can be used to derive the distribution of UCS and porosity between sampling sites, to upscale sample measurements to the rock mass scale (e.g., complementing m_i and Geological Strength Index - GSI), to resolve their spatial distribution, and, ultimately, to estimate critical rock failure parameters on a stratigraphical basis (e.g., Fig. 7A). Thus, in addition to being quick and non-destructive, we emphasize that our VNIR–SWIR spectroscopy approach can also provide a solution for gathering information on the heterogeneity of volcanic systems regardless of terrain or compositional, lithological, and alteration diversity.

Our UCS predictions on rock chips outperform predictions on rock powders, with only a moderate increase in model complexity (e.g., number of PLS components; Table 1). This highlights that hydrothermal and weathering-related alteration and its spatial variability within a sample, captured by VNIR–SWIR reflectance, can contribute positively to UCS predictions. This realisation presents a great opportunity for VNIR–SWIR spectroscopy to be used on in-situ rock surfaces without the need for extensive sample preprocessing and contributes to new applications to map physical and mechanical inhomogeneities from macroscopic to edifice length scales. The models produced herein use spectral measurements that represent whole-rock composition (internal and external portions). Because remotely sensed spectral imaging via aerial or satellite data can only capture the external portions of rocks or rock masses, model calibration may be required for upscaling efforts. However, the increasing availability of hyperspectral remote sensing data, from satellites (e.g., PRISMA), airborne (e.g., AVIRIS), or ground-based platforms (Kereszturi et al., 2018; Cogliati et al., 2021; Thiele et al., 2022), is opening new avenues for the mapping and analysis of alteration and volcano stability at volcanoes worldwide. Furthermore, remote sensing methods are important as partially lithified pyroclastic rocks (e.g., breccia-horizons and tephra) are often complicated and difficult to measure accurately in the laboratory (Schaefer et al., 2018) and are also subject to eruption-related porosity changes and thermal cracking (Vinciguerra et al., 2005; Heap and Violay, 2021; Kanakiya et al., 2021). Bridging

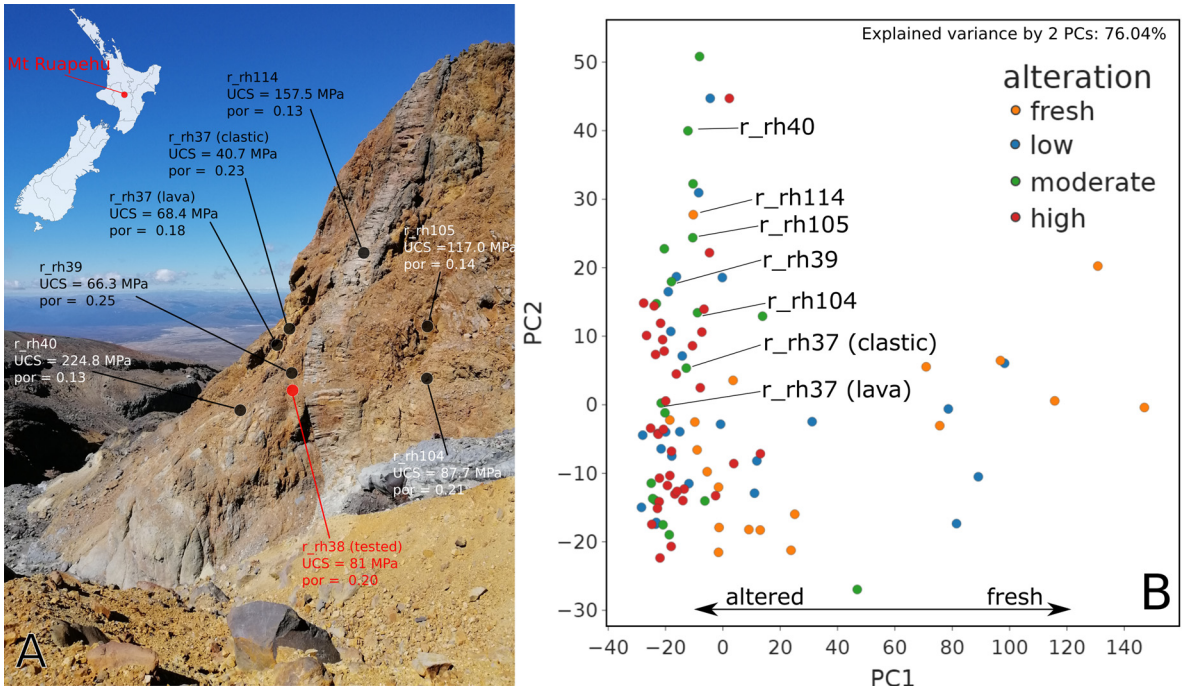

Fig. 7. Application of uniaxial compressive strength (UCS) and porosity models to a natural outcrop within the Wahianoa formation on Mt Ruapehu (top left inset shows a map of New Zealand with the location of Mt Ruapehu indicated). (A) Locations of samples collected for deriving spectroscopy-derived UCS and porosity (por) estimates (in black) around an intrusion surrounded by variably altered brecciated and coherent lava rocks. The sample locations are approximated. UCS and porosity of sample, r_rh38 (in red) were tested in the laboratory. (B) Plot showing the Principal Component 1 and 2 (PC1 and PC2, respectively) for the training data and the "unseen" samples that were predicted using the full dataset, including all volcanoes. Samples shown in (A) are labelled.

physio/mechanical predictions using remote sensing can be further developed in the future to improve model input parameters for slope stability assessments of volcanoes.

5. Conclusions

Hydrothermal alteration can both precipitate secondary minerals which occupy pore space and reduce porosity and increase overall porosity by dissolution (del Potro and Hürlimann, 2009; Heap et al., 2021b; Kanakiya et al., 2021), complicating UCS predictions using only porosity. Our results and models offer an improved prediction by combining porosity and spectroscopy data. Additionally, our models can distinguish between changes in UCS that result from porosity versus changes that result from hydrothermal alteration. This is due to the underlying sensitivity of the VNIR–SWIR spectroscopy via absorption features specific to alteration minerals.

Rock testing is critical to understanding the mechanical and physio-chemical characteristics of rocks (i.e., how a rock reacts when stressed). Their behaviour controls volcanic processes ranging from outgassing via hydrothermal fluid circulation to volcano deformation (Heap and Violay, 2021). However, laboratory rock testing is expensive, time-consuming, destructive and cannot be carried out in the field. Our new spectroscopy-only method can overcome these limitations by providing rapid remote sensing insights into the heterogeneity of mechanical behaviour of volcanic rocks. The presented approach can be used as a 'pre-screening' tool to optimize sampling campaigns and be potentially repurposed to upscale mechanical testing results (e.g., from samples/cores to rock mass) using spectral information from ground, airborne and satellite sensors.

The spectral-geotechnical database compiled here is limited, even though it contains samples representing a wide range of compositions and hydrothermal alteration styles. Although our results are consistent, the prediction models can be improved by benchmarking a range of prediction models, including adaptive boosting (e.g., Feng et al., 2020), or complementing VNIR-SWIR spectroscopy with portable X-Ray Fluorescence or Mid to Longwave Infrared spectroscopy (e.g., Shrestha et al., 2022). Furthermore, the database should be continually improved as and when new data become available, which will improve UCS and porosity predictions across rock types and compositional ranges. Developing a similar method to predict the Hoek-Brown parameter m_i would provide full failure criteria for intact rocks, which can be combined with remotely-obtained GSI values to numerically model the stability of rock masses. By resolving the heterogeneity of volcanic rocks, the statistically sound UCS and porosity predictions offered by the VNIR–SWIR spectroscopy approach, can resolve the heterogeneity of volcanic rock masses, improving near-surface slope failure assessments in volcanic environments.

CRediT authorship contribution statement

Gabor Kereszturi: Conceptualization, Data curation, Formal analysis, Funding acquisition, Investigation, Methodology, Project administration, Resources, Software, Validation, Writing – original draft. **Michael Heap:** Conceptualization, Investigation, Resources, Writing – original draft, Writing – review & editing. **Lauren N. Schaefer:** Conceptualization, Investigation, Resources, Writing – review & editing. **Herlan Darmawan:** Resources, Writing – review & editing. **Frances M. Deegan:** Resources, Writing – review & editing. **Ben Kennedy:** Resources, Writing – review & editing. **Jean-Christophe Komorowski:** Resources, Writing – review & editing. **Stuart Mead:** Software, Writing – review & editing. **Marina Rosas-Carbajal:** Resources, Writing – review & editing. **Amy Ryan:** Resources, Writing – review & editing. **Valentin R. Troll:** Resources, Writing – review & editing. **Marlène Villeneuve:** Resources, Writing – review & editing. **Thomas R. Walter:** Resources, Writing – review & editing.

Declaration of competing interest

The authors declare that they have no known competing financial interests or personal relationships that could have appeared to influence the work reported in this paper.

Data availability

All mechanical and spectral data has been shared as supplementary files, while the processing Python codes are available from the corresponding author upon request.

Acknowledgements

This research was supported by Natural Hazard Research Platform ("Too big to fail? A multidisciplinary approach to predict collapse and debris flow hazards from Mt. Ruapehu"; MAU-01-NHRP-31118) and partially through GK's Rutherford Discovery Fellowship ("Caught in action - volcano surveillance with hyperspectral remote sensing"; RDF-MAU2003). This work was supported in part by ANR grant MYGALE ("Modelling the phYsical and chemical Gradients of hydrothermal ALteration for warning systems of flank collapse at Explosive volcanoes"; ANR-21-CE49-0010), awarded to MJH, and by the Indonesia-German SUNDAARC agreement and represents a contribution to the programme GEOTECHNOLOGIEN by BMBF and DFG (Grant 03G0578A). MJH also acknowledges support from the Institut Universitaire de France (IUF) and FMD and VRT acknowledge support from the Swedish Research Council and the Section for Natural Resources and Sustainable Development (NRHU) at Uppsala University. BK and GK additionally acknowledges Ministry of Business, Innovation & Employment-funded National Science Challenges – Resilience to Nature's Challenges programme ("Āhea riri ai ngā maunga puia? When will our volcanoes become angry?"; GNS-RNC047).

Any use of trade, firm, or product names is for descriptive purposes only and does not imply endorsement by the U.S. Government.

Appendix A. Supplementary material

Supplementary material related to this article can be found online at https://doi.org/10.1016/j.epsl.2022.117929.

References

Apuani, T., Corazzato, C., Cancelli, A., Tibaldi, A., 2005. Physical and mechanical properties of rock masses at Stromboli: a dataset for volcano instability evaluation. Bull. Eng. Geol. Environ. 64 (4), 419.

Ball, J.L., Taron, J., Reid, M.E., Hurwitz, S., Finn, C., Bedrosian, P., 2018. Combining multiphase groundwater flow and slope stability models to assess stratovolcano flank collapse in the cascade range. J. Geophys. Res., Solid Earth 123 (4), 2787–2805.

Barzegar, R., Sattarpour, M., Nikudel, M.R., Moghaddam, A.A., 2016. Comparative evaluation of artificial intelligence models for prediction of uniaxial compressive strength of travertine rocks, case study: Azarshahr area, NW Iran. Model. Earth Syst. Environ. 2 (2), 76.

Bishop, J., Murad, E., Dyar, M.D., 2002. The influence of octahedral and tetrahedral cation substitution on the structure of smectites and serpentines as observed through infrared spectroscopy. Clay Miner. 37 (4), 617–628.

Bishop, J.L., Michalski, J.R., Carter, J., 2017. Chapter 14 - Remote detection of clay minerals. In: Gates, W.P., Kloprogge, J.T., Madejová, J., Bergaya, F. (Eds.), Developments in Clay Science. Elsevier, pp. 482–514.

Bubeck, A., Walker, R.J., Healy, D., Dobbs, M., Holwell, D.A., 2017. Pore geometry as a control on rock strength. Earth Planet. Sci. Lett. 457, 38–48.

Chong, I.-G., Jun, C.-H., 2005. Performance of some variable selection methods when multicollinearity is present. Chemom. Intell. Lab. Syst. 78 (1), 103–112.

Clark, R.N., King, T.V.V., Klejwa, M., Swayze, G.A., 1990. High spectral resolution reflectance spectroscopy of minerals. J. Geophys. Res. 95, 12653–12680.

Clark, R.N., Swayze, G.A., Livo, K.E., Kokaly, R.F., Sutley, S.J., Dalton, J.B., McDougal, R.R., Gent, C.A., 2003. Imaging spectroscopy: Earth and planetary remote sensing with the USGS Tetracorder and expert systems. J. Geophys. Res. E, Planets 108 (12), 1–44.

Cogliati, S., Sarti, F., Chiarantini, L., Cosi, M., Lorusso, R., Lopinto, E., Miglietta, F., Genesio, L., Guanter, L., Damm, A., Pérez-López, S., Scheffler, D., Tagliabue, G., Panigada, C., Rascher, U., Dowling, T.P.F., Giardino, C., Colombo, R., 2021. The PRISMA imaging spectroscopy mission: overview and first performance analysis. Remote Sens. Environ. 262, 112499.

Darmawan, H., Troll, V.R., Walter, T.R., Deegan, F.M., Geiger, H., Heap, M.J., Seraphine, N., Harris, C., Humaida, H., Müller, D., 2022. Hidden mechanical weaknesses within lava domes provided by buried high-porosity hydrothermal alteration zones. Sci. Rep. 12 (1), 3202.

Darmawan, H., Walter, T.R., Troll, V.R., Budi-Santoso, A., 2018. Structural weakening of the Merapi dome identified by drone photogrammetry after the 2010 eruption. Nat. Hazards Earth Syst. Sci. 18 (12), 3267–3281.

del Potro, R., Hürlimann, M., 2009. The decrease in the shear strength of volcanic materials with argillic hydrothermal alteration, insights from the summit region of Teide stratovolcano, Tenerife. Eng. Geol. 104 (1), 135–143.

Feng, D.-C., Liu, Z.-T., Wang, X.-D., Chen, Y., Chang, J.-Q., Wei, D.-F., Jiang, Z.-M., 2020. Machine learning-based compressive strength prediction for concrete: an adaptive boosting approach. Constr. Build. Mater. 230, 117000.

Fortin, J., Stanchits, S., Vinciguerra, S., Guéguen, Y., 2011. Influence of thermal and mechanical cracks on permeability and elastic wave velocities in a basalt from Mt. Etna volcano subjected to elevated pressure. Tectonophysics 503 (1), 60–74.

Frolova, J., Ladygin, V., Rychagov, S., Zukhubaya, D., 2014. Effects of hydrothermal alterations on physical and mechanical properties of rocks in the Kuril–Kamchatka island arc. Eng. Geol. 183, 80–95.

Gamble, J.A., Price, R.C., Smith, I.E.M., McIntosh, W.C., Dunbar, N.W., 2003. 40Ar/39Ar geochronology of magmatic activity, magma flux and hazards at Ruapehu volcano, Taupo Volcanic Zone, New Zealand. J. Volcanol. Geotherm. Res. 120 (3–4), 271–287.

Geshi, N., Kusumoto, S., Gudmundsson, A., 2012. Effects of mechanical layering of host rocks on dike growth and arrest. J. Volcanol. Geotherm. Res. 223–224, 74–82.

Giampiccolo, E., Cocina, O., De Gori, P., Chiarabba, C., 2020. Dyke intrusion and stress-induced collapse of volcano flanks: the example of the 2018 event at Mt. Etna (Sicily, Italy). Sci. Rep. 10 (1), 6373.

Griffiths, L., Heap, M.J., Xu, T., Chen, C.-f., Baud, P., 2017. The influence of pore geometry and orientation on the strength and stiffness of porous rock. J. Struct. Geol. 96, 149–160.

Harnett, C.E., Heap, M.J., 2021. Mechanical and topographic factors influencing lava dome growth and collapse. J. Volcanol. Geotherm. Res. 420, 107398.

Harnett, C.E., Thomas, M.E., Purvance, M.D., Neuberg, J., 2018. Using a discrete element approach to model lava dome emplacement and collapse. J. Volcanol. Geotherm. Res. 359, 68–77.

Heap, M.J., Baumann, T., Gilg, H.A., Kolzenburg, S., Ryan, A.G., Villeneuve, M., Russell, J.K., Kennedy, L.A., Rosas-Carbajal, M., Clynne, M.A., 2021a. Hydrothermal alteration can result in pore pressurization and volcano instability. Geology 49 (11), 1348–1352.

Heap, M.J., Baumann, T.S., Rosas-Carbajal, M., Komorowski, J.-C., Gilg, H.A., Villeneuve, M., Moretti, R., Baud, P., Carbillet, L., Harnett, C., Reuschlé, T., 2021b. Alteration-induced Volcano Instability at La Soufrière de Guadeloupe (Eastern Caribbean). J. Geophys. Res., Solid Earth 126 (8), e2021JB022514.

Heap, M.J., Gravley, D.M., Kennedy, B.M., Gilg, H.A., Bertolett, E., Barker, S.L.L., 2020. Quantifying the role of hydrothermal alteration in creating geothermal and epithermal mineral resources: the Ohakuri ignimbrite (Taupō Volcanic Zone, New Zealand). J. Volcanol. Geotherm. Res. 390, 106703.

Heap, M.J., Kennedy, B.M., Farquharson, J.I., Ashworth, J., Mayer, K., Letham-Brake, M., Reuschlé, T., Gilg, H.A., Scheu, B., Lavallée, Y., Siratovich, P., Cole, J., Jolly, A.D., Baud, P., Dingwell, D.B., 2017. A multidisciplinary approach to quantify the permeability of the Whakaari/White Island volcanic hydrothermal system (Taupo Volcanic Zone, New Zealand). J. Volcanol. Geotherm. Res. 332, 88–108.

Heap, M.J., Kennedy, B.M., Pernin, N., Jacquemard, L., Baud, P., Farquharson, J.I., Scheu, B., Lavallée, Y., Gilg, H.A., Letham-Brake, M., Mayer, K., Jolly, A.D., Reuschlé, T., Dingwell, D.B., 2015. Mechanical behaviour and failure modes in the Whakaari (White Island volcano) hydrothermal system, New Zealand. J. Volcanol. Geotherm. Res. 295, 26–42.

Heap, M.J., Troll, V.R., Harris, C., Gilg, H.A., Moretti, R., Rosas-Carbajal, M., Komorowski, J.-C., Baud, P., 2022. Whole-rock oxygen isotope ratios as a proxy for the strength and stiffness of hydrothermally altered volcanic rocks. Bull. Volcanol. 84 (8), 74.

Heap, M.J., Troll, V.R., Kushnir, A.R.L., Gilg, H.A., Collinson, A.S.D., Deegan, F.M., Darmawan, H., Seraphine, N., Neuberg, J., Walter, T.R., 2019. Hydrothermal alteration of andesitic lava domes can lead to explosive volcanic behaviour. Nat. Commun. 10 (1), 5063.

Heap, M.J., Violay, M.E.S., 2021. The mechanical behaviour and failure modes of volcanic rocks: a review. Bull. Volcanol. 83 (5), 33.

Hoek, E., Brown, E.T., 1997. Practical estimates of rock mass strength. Int. J. Rock Mech. Min. Sci. 34 (8), 1165–1186.

Hunt, G., 1977. Spectral signatures of particulate minerals in the visible and near infrared. Geophysics 42.

Jahed Armaghani, D., Mohd Amin, M.F., Yagiz, S., Faradonbeh, R.S., Abdullah, R.A., 2016a. Prediction of the uniaxial compressive strength of sandstone using various modeling techniques. Int. J. Rock Mech. Min. Sci. 85, 174–186.

Jahed Armaghani, D., Tonnizam Mohamad, E., Hajihassani, M., Yagiz, S., Motaghedi, H., 2016b. Application of several non-linear prediction tools for estimating uniaxial compressive strength of granitic rocks and comparison of their performances. Eng. Comput. 32 (2), 189–206.
Kanakiya, S., Adam, L., Rowe, M.C., Lindsay, J.M., Esteban, L., 2021. The role of tuffs in sealing volcanic conduits. Geophys. Res. Lett. 48 (20), e2021GL095175.
Kaufman, S., Rosset, S., Perlich, C., 2011. Leakage in Data Mining: Formulation, Detection, and Avoidance. KDD.
Kendrick, J.E., Smith, R., Sammonds, P., Meredith, P.G., Dainty, M., Pallister, J.S., 2013. The influence of thermal and cyclic stressing on the strength of rocks from Mount St. Helens, Washington. Bull. Volcanol. 75 (7), 728.
Kereszturi, G., Schaefer, L., Mead, S., Miller, C., Procter, J., Kennedy, B., 2021. Synthesis of hydrothermal alteration, rock mechanics and geophysical mapping to constrain failure and debris avalanche hazards at Mt. Ruapehu (New Zealand). N.Z. J. Geol. Geophys. 64 (2–3), 421–442.
Kereszturi, G., Schaefer, L.N., Miller, C., Mead, S., 2020. Hydrothermal alteration on composite volcanoes: mineralogy, hyperspectral imaging, and aeromagnetic study of Mt Ruapehu, New Zealand. Geochem. Geophys. Geosyst. 21 (9), e2020GC009270.
Kereszturi, G., Schaefer, L.N., Schleiffarth, W.K., Procter, J., Pullanagari, R.R., Mead, S., Kennedy, B., 2018. Integrating airborne hyperspectral imagery and LiDAR for volcano mapping and monitoring through image classification. Int. J. Appl. Earth Obs. Geoinf. 73, 323–339.
Kokaly, R.F., Clark, R.N., Swayze, G.A., Livo, K.E., Hoefen, T.M., Pearson, N.C., Wise, R.A., Benzel, W.M., Lowers, H.A., Driscoll, R.L., Klein, A.J., 2017. USGS Spectral Library Version 7. 1035, Reston, VA.
Loughlin, W.P., 1991. Principal component analysis for alteration mapping. Photogramm. Eng. Remote Sens. 57 (9), 1163–1169.
Madejová, J., Gates, W.P., Petit, S., 2017. Chapter 5 - IR spectra of clay minerals. In: Gates, W.P., Kloprogge, J.T., Madejová, J., Bergaya, F. (Eds.), Developments in Clay Science. Elsevier, pp. 107–149.
Manconi, A., Walter, T.R., Amelung, F., 2007. Effects of mechanical layering on volcano deformation. Geophys. J. Int. 170 (2), 952–958.
Mordensky, S.P., Heap, M.J., Kennedy, B.M., Gilg, H.A., Villeneuve, M.C., Farquharson, J.I., Gravley, D.M., 2019. Influence of alteration on the mechanical behaviour and failure mode of andesite: implications for shallow seismicity and volcano monitoring. Bull. Volcanol. 81 (8), 44.
Mordensky, S.P., Villeneuve, M.C., Farquharson, J.I., Kennedy, B.M., Heap, M.J., Gravley, D.M., 2018a. Rock mass properties and edifice strength data from Pinnacle Ridge, Mt. Ruapehu, New Zealand. J. Volcanol. Geotherm. Res. 367, 46–62.
Mordensky, S.P., Villeneuve, M.C., Kennedy, B.M., Heap, M.J., Gravley, D.M., Farquharson, J.I., Reuschlé, T., 2018b. Physical and mechanical property relationships of a shallow intrusion and volcanic host rock, Pinnacle Ridge, Mt. Ruapehu, New Zealand. J. Volcanol. Geotherm. Res. 359, 1–20.
Mordensky, S.P., Villeneuve, M.C., Kennedy, B.M., Struthers, J.D., 2022. Hydrothermally induced edifice destabilisation: the mechanical behaviour of rock mass surrounding a shallow intrusion in andesitic lavas, Pinnacle Ridge, Ruapehu, New Zealand. Eng. Geol. 305, 106696.
Müller, D., Bredemeyer, S., Zorn, E., De Paolo, E., Walter, T.R., 2021. Surveying fumarole sites and hydrothermal alteration by unoccupied aircraft systems (UAS) at the La Fossa cone, Vulcano Island (Italy). J. Volcanol. Geotherm. Res. 413, 107208.
Neal, L.C., Wilkinson, J.J., Mason, P.J., Chang, Z., 2018. Spectral characteristics of propylitic alteration minerals as a vectoring tool for porphyry copper deposits. J. Geochem. Explor. 184, 179–198.
Pedregosa, F., Varoquaux, G., Gramfort, A., Michel, V., Thirion, B., Grisel, O., Blondel, M., Prettenhofer, P., Weiss, R., Dubourg, V., Vanderplas, J., Passos, A., Cournapeau, D., Brucher, M., Perrot, M., Duchesnay, E., 2011. Scikit-learn: machine learning in Python. J. Mach. Learn. Res. 12, 2825–2830.
Pola, A., Crosta, G., Fusi, N., Barberini, V., Norini, G., 2012. Influence of alteration on physical properties of volcanic rocks. Tectonophysics 566–567, 67–86.
Reid, M.E., 2004. Massive collapse of volcano edifices triggered by hydrothermal pressurization. Geology 32 (5), 373–376.
Reid, M.E., Keith, T.E.C., Kayen, R.E., Iverson, N.R., Iverson, R.M., Brien, D.L., 2010. Volcano collapse promoted by progressive strength reduction: new data from Mount St. Helens. Bull. Volcanol. 72 (6), 761–766.
Reid, M.E., Sisson, T.W., Brien, D.L., 2001. Volcano collapse promoted by hydrothermal alteration and edifice shape, Mount Rainier, Washington. Geology 29 (9), 779–782.
Revil, A., Qi, Y., Panwar, N., Gresse, M., Grandis, H., Sharma, R., Géraud, Y., Chibati, N., Ghorbani, A., 2022. Induced polarization images alteration in stratovolcanoes. J. Volcanol. Geotherm. Res. 429, 107598.
Rowan, L.C., Hook, S.J., Abrams, M.J., Mars, J.C., 2003. Mapping hydrothermally altered rocks at Cuprite, Nevada, using the Advanced Spaceborne Thermal Emission and Reflection Radiometer (ASTER), a new satellite-imaging system. Econ. Geol. 98.
Savitzky, A., Golay, M.J.E., 1964. Smoothing and differentiation of data by simplified least squares procedures. Anal. Chem. 36 (8), 1627–1639.
Schaefer, L.N., Kendrick, J.E., Oommen, T., Lavallée, Y., Chigna, G., 2015. Geomechanical rock properties of a basaltic volcano. Front. Earth Sci. 3 (29).
Schaefer, L.N., Kennedy, B.M., Villeneuve, M.C., Cook, S.C.W., Jolly, A.D., Keys, H.J.R., Leonard, G.S., 2018. Stability assessment of the Crater Lake/Te Wai-ā-moe overflow channel at Mt. Ruapehu (New Zealand), and implications for volcanic lake break-out triggers. J. Volcanol. Geotherm. Res. 358, 31–44.
Schaefer, L.N., Kereszturi, G., Kennedy, B., Villeneuve, M., 2022. Characterizing lithological, weathering, and hydrothermal alteration influences on volcanic rock properties via spectroscopy and laboratory testing: a case study of Mt. Ruapehu volcano, New Zealand. Bull. Volcanol. https://doi.org/10.1002/essoar.10504173.1, submitted for publication.
Schaefer, L.N., Kereszturi, G., Villeneuve, M., Kennedy, B., 2021. Determining physical and mechanical volcanic rock properties via reflectance spectroscopy. J. Volcanol. Geotherm. Res. 420, 107393.
Schaefer, L.N., Oommen, T., Corazzato, C., Tibaldi, A., Escobar-Wolf, R., Rose, W.I., 2013. An integrated field-numerical approach to assess slope stability hazards at volcanoes: the example of Pacaya, Guatemala. Bull. Volcanol. 75 (6), 720.
Shrestha, G., Calvelo-Pereira, R., Roudier, P., Martin, A.P., Turnbull, R.E., Kereszturi, G., Jeyakumar, P., Anderson, C.W.N., 2022. Quantification of multiple soil trace elements by combining portable X-ray fluorescence and reflectance spectroscopy. Geoderma 409.
Thiele, S.T., Bnoulkacem, Z., Lorenz, S., Bordenave, A., Menegoni, N., Madriz, Y., Dujoncquoy, E., Gloaguen, R., Kenter, J., 2022. Mineralogical mapping with accurately corrected shortwave infrared hyperspectral data acquired obliquely from UAVs. Remote Sens. 14 (1), 5.
van Wyk de Vries, B., Kerle, N., Petley, D., 2000. Sector collapse forming at Casita volcano, Nicaragua. Geology 28 (2), 167–170.
Vasseur, J., Wadsworth, F.B., 2019. The permeability of columnar jointed lava. J. Geophys. Res., Solid Earth 124 (11), 11305–11315.
Villeneuve, M.C., Heap, M.J., 2021. Calculating the cohesion and internal friction angle of volcanic rocks and rock masses. Volcanica 4 (2), 279–293.
Vinciguerra, S., Trovato, C., Meredith, P.G., Benson, P.M., 2005. Relating seismic velocities, thermal cracking and permeability in Mt. Etna and Iceland basalts. Int. J. Rock Mech. Min. Sci. 42 (7), 900–910.
Wallace, C.S., Schaefer, L.N., Villeneuve, M.C., 2022. Material properties and triggering mechanisms of an andesitic lava dome collapse at Shiveluch Volcano, Kamchatka, Russia, revealed using the finite element method. Rock Mech. Rock Eng. 55 (5), 2711–2728.
Wold, S., Sjöström, M., Eriksson, L., 2001. PLS-regression: a basic tool of chemometrics. Chemom. Intell. Lab. Syst. 58 (2), 109–130.